

## Progress and current state of the art of Diamond-based MESFETs

R S Balmer, I Friel, M Schwitters, S Woollard, C J H Wort, G A Scarsbrook, S E Coe  
Element Six Ltd, King's Ride Park,  
Ascot, UK. SL5 8BP

H El-Hajj, A Kaiser, A Denisenko, E Kohn  
Department of Electron Devices and Circuits,  
University of Ulm, Germany

### Abstract

*In this paper we review the progress on diamond based MESFETs for high frequency, high power applications. The principle challenges of realising these devices are discussed and results presented which represent the current state of the art for delta-layer diamond MESFETs. Transistor characteristics for a single delta device are reported showing a current density  $>30$  mA/mm along with small signal RF measurements demonstrating GHz operation.*

Keywords: Diamond, CVD, doping, microwave, MESFET

### Introduction

Due to physical limitations, silicon and gallium arsenide devices are unlikely to achieve power levels higher than a few hundreds of watts depending on the frequency to be amplified. Wide bandgap materials, in principle, allow for higher power output per unit gate length at microwave frequencies. This is because a larger bias voltage, and hence the voltage amplitude on the microwave signal, can be supported across the transistor channel region over which the current is modulated. This is made possible by the high breakdown electric fields of wide bandgap semiconductors.

In microwave power transistors, the ability to support high voltage is particularly desirable, since power is typically transferred to a relatively high impedance (e.g.  $50 \Omega$ ) load. Diamond, with its extreme physical properties, may enable a real breakthrough by allowing the replacement of high power vacuum tube devices by solid-state components. If the

intrinsic properties of diamond can be fully exploited through novel device design and fabrication, diamond devices could take the entire RF generation market up to 100 GHz.

### CVD Diamond As An Electronic Material

Diamond is extreme in the group of wide bandgap materials that includes silicon carbide (SiC) and gallium nitride (GaN). Diamond electronic devices, such as power diodes and high-frequency field effect transistors, are expected to deliver outstanding performance due to the material's excellent intrinsic properties, as summarised in Figure 1.

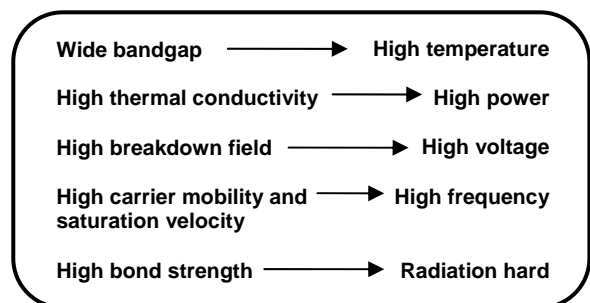


**Figure 1.** Important material properties of single crystal CVD diamond which make it an ideal candidate for high power, high frequency electronic devices.

It is the unmatched combination of highest bulk thermal conductivity, high carrier mobility and high breakdown voltage that make diamond a truly multifunctional material and will allow applications in environments simply too demanding for other materials and devices. However, the high activation energies of dopants in diamond makes it necessary to explore less conventional device designs, such as delta-doped FETs with very highly doped regions separated from the active region of the device.

### Doping Of CVD Diamond

Dopants in wide bandgap semiconductors tend to have higher ionisation energies than those in narrow bandgap semiconductors, resulting in low activation at room temperature. For example, 4H-SiC has shallow donors (n-dopant), but lacks a shallow acceptor (p-dopant), the shallowest being aluminium with ionisation energy of 0.19 eV [1]. In the case of diamond, known dopants have even higher ionisation energies. The most common dopants used in diamond are listed in Table 1 with their associated ionisation energy.

**Table 1.** Common dopants in CVD diamond.

|        | Element     | Activation Energy (eV) |
|--------|-------------|------------------------|
| N-type | Nitrogen    | 1.7                    |
|        | Phosphorous | 0.6 [2]                |
| P-type | Boron       | 0.37                   |

Reports claiming that sulphur (S) or oxygen (O) constitute reasonably shallow donors remain to be substantiated at the time of writing. A boron-hydrogen complex has also recently been reported to constitute a reasonably shallow n-dopant [3], but the long-term stability of this complex is uncertain. As boron is readily incorporated

into CVD diamond as a dopant impurity, there has been much activity focused on unipolar devices using boron. However, boron acceptors are only weakly activated at room temperature due to the ionisation energy of 0.37 eV. To mitigate this, the boron solid concentration must be increased to very high levels where the conduction mechanism changes first from band type conduction to hopping then eventually to metallic-like as the acceptor bands begin to overlap the valence band maximum and the activation energy approaches zero (the Mott transition). At the same time, the presence of compensating donors (shallow or deep) must be minimised. This metallic-like conduction results in much lower bulk resistivity.

### MESFET For High Power, High Frequency Applications

A conventional MESFET device design is shown diagrammatically in Figure 2. Ohmic current transport takes place between the source and drain contacts until the saturation velocity,  $v_{sat}$  is reached. The maximum channel current  $J$  is proportional to  $qN_A t v_{sat}$ , where  $t$  is the channel thickness and  $N_A$  is the acceptor concentration. But to be in the metallic conduction regime requires that  $N_A > 10^{20} \text{ cm}^{-3}$  which would mean that the mobility of holes in the channel is significantly degraded due to ionised impurity scattering.

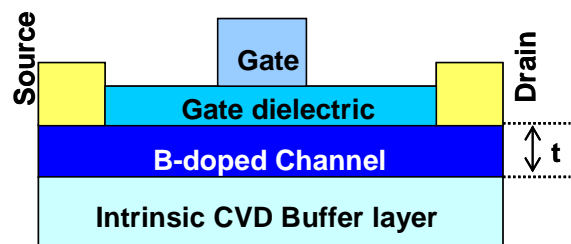


**Figure 2.** Basic unipolar device design: Doped Channel Diamond MISFET.

Thus, because of the high ionisation energy of boron doped diamond, conventional device designs cannot be expected to yield high performance RF devices. Instead a

more creative approach to device design is required in order to utilise the superior properties of intrinsic diamond. In particular, it would be highly desirable to achieve some degree of spatial separation between ionised acceptors and holes. Several workers have made use of the unique ability in diamond to create a conductive (p-type) layer on the H-terminated surface (so-called ‘surface transfer doping’). We do not discuss surface devices in this paper, but impressive progress has been made by several groups with headline figures which include an output power density of  $2.1 \text{ Wmm}^{-1} \text{ cw}$  at 1 GHz ( $V_{DS}=-16 \text{ V}$ ,  $L_g=0.3 \mu\text{m}$ ,  $W_g=2 \times 50 \mu\text{m}$ ) [4] and  $F_t=45 \text{ GHz}$  and  $F_{max}=120 \text{ GHz}$  ( $V_{DS}=-18 \text{ V}$ ,  $L_g=0.1 \mu\text{m}$ ,  $W_g=50 \mu\text{m}$ ) [5]. Although these results are promising, the long term stability of these surface FETs remains an issue, particularly at elevated temperatures and in harsh environments.

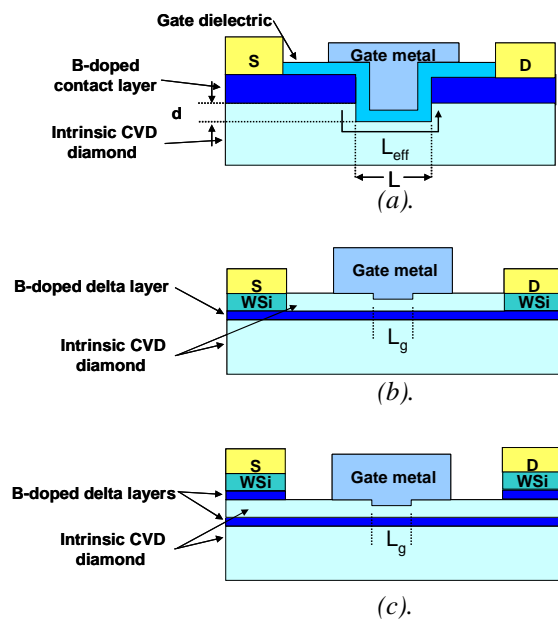


**Figure 3.** MESFET design concepts: (a) *P-i-P MISFET* (b) *delta MESFET* (c) *double-delta MESFET*.

### *P-i-P FET*

Alternative design concepts that have been investigated and which aim to utilise charge transport in intrinsic CVD diamond are shown diagrammatically in Figure 3. The

*P-i-P MISFET* design is similar to the basic design shown in Figure 2, except that a trench is etched through the doped conducting channel. Gate dielectric and metal are deposited into the trench as shown in Figure 3(a). This design was pioneered by Kobe Steel [6] based on space-charge ideas discussed in [7]. The current that flows around the gate is space-charge limited, which is not ideal for a high power transistor. Furthermore, successful operation requires very precise etching of the gate trench with nanometer control as the source-drain current is highly sensitive to the effective gate length ( $L_{eff}$ ).

### Delta FET

A more attractive design is shown in Figure 3(b) which separates the holes and ionised acceptors by incorporating a ‘delta’ doping layer, a technique pioneered in silicon devices and commonly used in III-V devices. The delta layer is a very thin (a few monolayers ideally) highly boron doped region sandwiched between ‘undoped’ intrinsic diamond. Most of the conduction occurs in the intrinsic layers due to diffusion of holes from the narrow delta-doped layer. The mobility in the delta layer with a doping concentration of  $10^{20} \text{ cm}^{-3}$  would be in the region of  $10 \text{ cm}^2\text{V}^{-1}\text{s}^{-1}$ , whereas it may be as high as  $3800 \text{ cm}^2\text{V}^{-1}\text{s}^{-1}$  in the intrinsic regions. Quantum-mechanical calculations predict that for a delta-layer thickness of 2 nm, 95% of the hole transport will take place above the delta layer in the intrinsic channel [8]. An enhanced variant of the single-delta MESFET is the double-delta MESFET shown in Figure 3(c). Here an additional boron doped layer is deposited on top of the structure which is used to make contact to the delta-layer and thus improve the source and drain ohmic contact properties.

Whilst offering performance advantages, the delta-layer design presents formidable synthesis challenges. Principal amongst these are the requirements to prepare atomically smooth diamond surfaces free of

damage, and the growth of nm-thin layers with atomically abrupt interfaces. This is challenging in any material, but for diamond grown by microwave CVD, it is particularly complicated due to the presence of the plasma and the difficulty of preparing a flat and smooth substrate surface.

### Substrate Preparation

Synthetic diamond substrate manufacture inevitably involves several processing steps in order to produce a basic substrate which is of a standard size (edge length and thickness). For a transistor structure containing a delta-layer, it is important that the substrate has an acceptably low surface roughness, since if the initial roughness is too great it may be impossible to prepare a low roughness surface for deposition of the delta layer. Element Six has considerable expertise in preparing diamond surfaces and has recently refined a polishing process specifically for electronics applications. This is a multi-step process capable of producing surfaces with rms roughness less than 0.2 nm. Figure 4 shows AFM images of a substrate surface taken at each stage of the polishing process. It can be seen that after the final stage, the rms roughness is reduced to less than 0.2 nm over both a  $2 \times 2$  and  $10 \times 10 \mu\text{m}$  area.

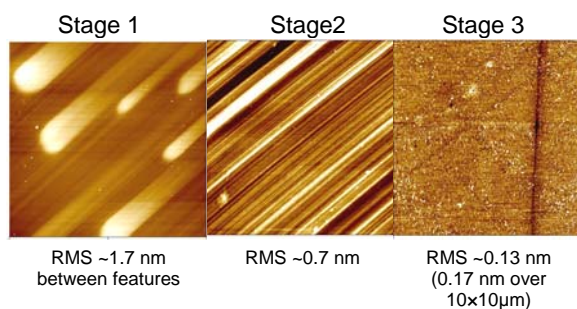


**Figure 4.** Height contrast AFM images of each stage of polishing process for producing ultra-smooth surfaces.

### Growth And Preparation Of Intrinsic Buffer Layer Surface

Of equal importance for the delta-layer MESFET design is the requirement to grow

the intrinsic buffer layer such that the surface is atomically smooth, in preparation for the boron delta-layer growth. For holes moving laterally in the intrinsic regions either side of the delta layer, any disorder in the interface between the two regions produces random potential energy fluctuations. These fluctuations lead to carrier scattering and hence a decrease in the mobility. At worst, for relatively high levels of roughness, carriers could become localised. We have therefore focussed on preparing low roughness surfaces via growth.

It was recognised that an as-grown surface with atomic-scale steps separated by atomically flat terraces would be an ideal starting surface on which to deposit a delta-layer. As such the conditions for achieving step-flow growth were investigated. It was found that by reducing the methane concentration, step-flow growth was initiated, as shown in Figure 5.

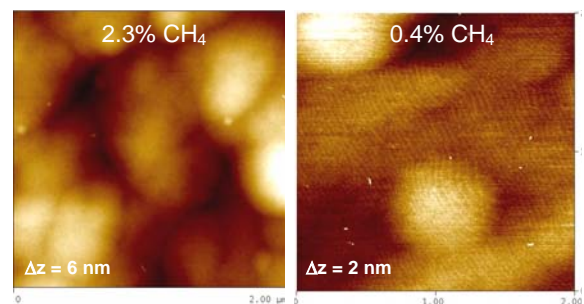


**Figure 5.**  $2 \times 2 \mu\text{m}$  height contrast AFM images of as-grown CVD diamond surfaces illustrating the transition to step-flow growth for low  $\text{CH}_4$  levels. A terraced surface is observed for a methane concentration of 0.4% indicating a transition to step-flow growth.

However, for these samples it was also found that low methane levels lead to a poor surface on the macroscopic scale, as illustrated in Figure 6. Work is on-going to optimise growth conditions to simultaneously produce surfaces which are atomically smooth on the microscopic scale whilst free from pits and hillocks on a macroscopic scale.

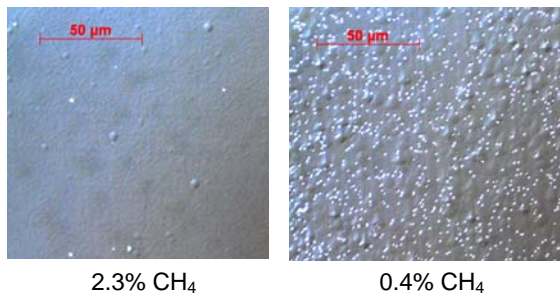


**Figure 6.** Corresponding optical microscopy (Nomarski) images of the samples shown in Figure 5.

### Boron Delta-Layer Growth

Secondary ion mass spectrometry (SIMS) is commonly used to assess the boron concentration in doped diamond layers. Figure 7 shows boron profiles from SIMS analysis of two delta layer structures grown by microwave CVD.

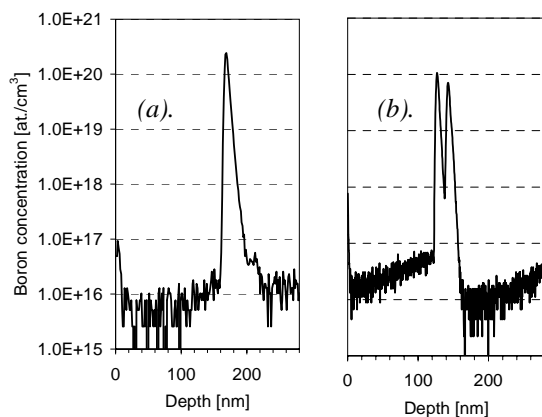


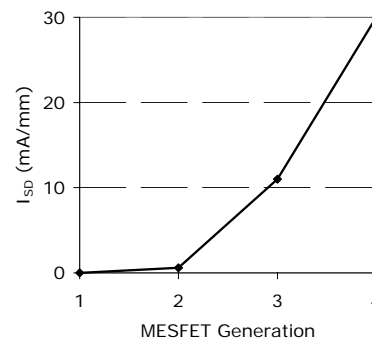
**Figure 7.** SIMS data for boron doped delta layers: (a) single-delta structure (b) double-delta structure.

Profile (a) is a single-delta structure and profile (b) is a double-delta structure. By careful tuning and optimisation of the growth conditions, a very abrupt rising edge (nearest the surface) of the doping peak is observed in both cases, with a gradient of 1 nm per decade of boron concentration. The asymmetry observed may be an artefact of the SIMS measurement. There are three important points to note with these profiles: firstly the peak boron concentration is  $\sim 10^{20}$  at.cm<sup>-3</sup> which is crucial for carrier activation at room temperature; secondly,

the interfaces are very abrupt and the peaks are narrow; and thirdly, the boron concentration in the material either side of the doping spike is low (close to SIMS background).

### Device Fabrication and Testing

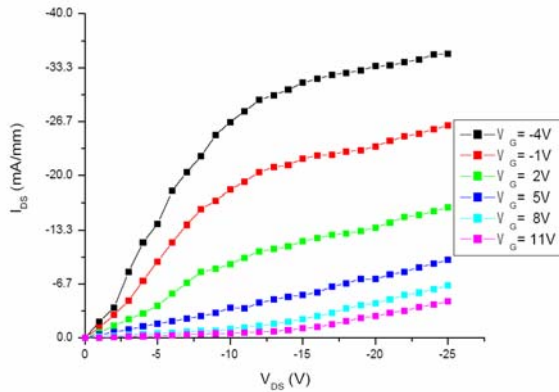
Steady progress on developing all the necessary building blocks to realise stable, high frequency diamond-based transistors has been made since 2004 (Figure 8). Although early prototype *P-i-P* transistors have been fabricated that demonstrate full pinch-off and basic transistor action even at significantly elevated temperatures (500K), it is currently believed that the delta-doped devices are a more practical route forward to realise high power at high frequencies.



**Figure 8.** Evolution of delta MESFET source-drain current.

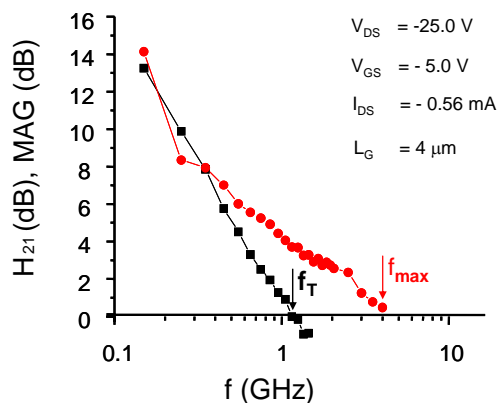
Devices have been fabricated on single delta structures using aluminium as the gate metal and precise etching of the top intrinsic diamond cap layer was employed to create ohmic contacts to the delta layer using a tungsten silicide metallisation scheme.

Figure 9 shows a room temperature DC output characteristic for a single delta device demonstrating a peak output current density of  $>30$  mA/mm. The channel is fully pinched off at lower source-drain voltages, but at higher bias the observed leakage current indicates that carrier conduction may be occurring through the substrate.



**Figure 9.** DC output characteristic for a single delta device with  $L_G=0.7 \mu\text{m}$  and  $W_G=30 \mu\text{m}$  measured at room temperature.

Small signal RF measurements have been performed on single delta devices. Figure 10 shows data extracted from S-parameters for one such device which demonstrates very promising results for the cut-off frequency,  $f_T > 1 \text{ GHz}$  and the maximum frequency of operation,  $f_{max} \sim 4 \text{ GHz}$ .



**Figure 10.** Small signal RF performance extracted from S-parameters for a single-delta structure showing a cut-off frequency  $F_T > 1 \text{ GHz}$  and the maximum frequency of operation  $F_{max} \sim 4 \text{ GHz}$ .

### Summary

The extreme properties of diamond make single crystal CVD diamond an attractive material for high power and high frequency electronic device applications. Element Six and the University of Ulm are developing synthesis and device fabrication processes

in order to achieve a high performance diamond microwave transistor. To date, the focus of the work has been based on a delta-layer device design. Progress towards realising a device with RF performance has encountered several significant technical challenges, however, recent developments indicate an encouraging future for diamond electronics.

### Acknowledgements

The work reported in this paper was funded by the Electro-Magnetic Remote Sensing (EMRS) Defence Technology Centre, established by the UK Ministry of Defence and run by a consortium SELEX Sensors and Airborne Systems, Thales Defence, Roke Manor Research and Filtronic.

### References

1. M. Ikeda, H. Matsunami, T. Tanaka, *Physical Review B*, **22**, 2842-2854 (1980).
2. M. Suzuki, S. Koizumi, M. Katagiri, H. Yoshida, N. Sakuma, T. Ono, T. Sakai. *Diamond and Related. Materials* **13** 2037 (2004).
3. J. Chevallier, F. Jomard, Z. Teukam, S. Koizumi, H. Kanda, Y. Sato, A. Deneuve, M. Bernard, *Diamond and Related. Materials* **11**, 1566-1571 (2002).
4. Hiram et al., Waseda University Tokyo Proceedings of ISPSD06, Naples, Italy (2006).
5. K. Ueda, M. Kasu, Y. Yamauchi, T. Makimoto, M. Schwitters, D.J. Twitchen, G.A. Scarsbrook, S.E. Coe, *IEEE Electron Device Letters*, **27**, 570 (2006).
6. N. Kawakami, Y. Yokota, T. Tachibana, K. Hayashi, K. Kobashi, *Diamond and Related. Materials* **14**, 509-513 (2005).
7. J. Isberg, J. Hammersberg, E. Johansson, T. Wikstrom, D.J. Twitchen, A.J. Whitehead, S.E. Coe, G.A. Scarsbrook, *Science* **297**, 1670-1672 (2002).
8. A. Denisenko. Private communication, Nov. (2006).